CHEMICAL ENGINEERING TRANSACTIONS
VOL. 46, 2015
A publication of AIDIC
The Italian Association of Chemical Engineering
Online at www.aidic.it/cet
Guest Editors: Peiyu Ren, Yancang Li, Huiping Song

ISBN 978-88-95608-37-2; **ISSN** 2283-9216
DOI: 10.3303/CET1546134

Model Test Study on Landslide Treatment With Unequally Spaced Single Row Steel Pipe Anti-sliding Pile

Zhao-jun Chu[*a, b], Jian-hu Sun[a], Zi-peng Chen[a], Wei-ming Luo[a]

[a]Department of Architecture & Civil Engineering, Logistical University Engineering, Chongqing 401311, China
[b] Chongqing Key Laboratory of Geomechanics & Geoenvironmental Protection, Chongqing 401311, China
410140@qq.com

By using the large physical test to analyze the mechanical effects of the anti-sliding pile towards the slope, this research can analyze the displacement of the top, cut export and the moment. Besides, the changeable rule about the change of the load and the soil pressure and the destruction of slope can be observed and analyzed. The results show that, during the process, the back of the pile top began to separate with the sliding body. Behind the pile, the anchoring section where near the sliding surface also separated with the sliding bed, generating a pumping area. Loading up to the 420kN, the horizontal displacement began to increase rapidly, and when load was 480kN, the horizontal displacement in the cut export also began to grow quickly. The bending moment of the pile distributed in apparent anti-S. The maximum moment of the anti-sliding section is in the place 48cm above the sliding surface. The maximum moment of anchoring section is located under the surface about 22cm deep. The maximum moment of the anti-sliding section is bigger than the value of the anchoring. Furthermore, both the back of the anti-sliding section and the front side of anchoring section are carrying loads in tension. The maximum soil pressure in front of the anti-sliding pile is located in 70cm above the sliding surface. The maximum soil pressure of the anchoring section is near the surface, but this value is zero in the bottom of the pile. In the back of the anti-sliding pile, the maximum soil pressure is in the 40cm above the surface. The soil pressure is bigger in the anchoring section, and the value in the surface is zero. The rule of distribution of the soil pressure apparently opposites with the rule in the back of the pile. The results can provide the design and calculation of the anti-sliding single steel pile some references.

1. Introduction

In order to prevent the slope slide, the most effective mean of handling the landslide is to set the anti-sliding retaining structure. Among them, the application of anti-slide pile is more extensive(Ashour and Ardalan 2012; Xu and Niu 2014). However, the normal anti-sliding pile made of reinforced concrete has big cross-sectional area and is slow to construct. Moreover, with the big quantity , expensive cost, low security , it can hardly meet the requirements of the quickness in landslide prevention, safety and economy. Since the steel pipe anti-sliding pile can construct quickly and easily adapt to the site, it is really suitable for the landslide engineering repairment, with its high security, recoverability (Bruce et al 2005; Zhang and Tan 2013; Yan et al 2009; Gong et al 2004).

At present, domestic and overseas scholars are doing mechanical effect researches mainly on small size independence design. However, the research objects mainly are equally spaced arrangement's concrete pile(Poulos et al 1995; Xin et al 2014; Kong et al 2013; Li et al 2009; IAI 1989). The devices are small model casings instead of large-scale ones. Also, in order to to simulate the landslide thrust towards the anti-sliding pile, most of the model tests were inflicted horizontal loads to the model pile through jack, which is different from practical circumstance. This paper carry on mechanics effect research of unequally spaced single row steel pipe anti-sliding pile through a large scale of physical model test, obtain variation outcomes circumstances of displacement of pile top, displacement of landslide shear crack, bending along pile shaft, radial soil pressure around pile through loading change. In addition, provide test foundation for the design of steel pipe anti-sliding pile through observing pile body and damages of landslide. For purposes of discussion, the front side is the side which the pile closing to slope toe, and the back side is close to slope crest.

Please cite this article as: Chu Z.J., Sun J.H., Chen Z.P., Luo W.M., 2015, Model test study on landslide treatment with unequally spaced single row steel pipe anti-sliding pile, Chemical Engineering Transactions, 46, 799-804 DOI:10.3303/CET1546134

2. Design of Model Test

2.1 Intention of Test

By using the large physical test to analyze the mechanical effects of the single row steel pipe anti-sliding pile towards the slope, this research can analyze the displacement of the top, cut export and the moment. Besides, the changeable rule about the change of the load and the soil pressure and the destruction of slope can be observed and analyzed.

2.2The Design of The Similar Ratio About The Model Test

Taking the geometric similarity ratio as 1:6 and using the elastic modulus ratio as 1:1, this paper can figure out that C_q=1/6,C_P=1/36,C_σ=1,C_ε=1,C_{Ac}=1/36,C_γ=6 by similar theories(Lei et al 2007; Zhou et al 2005). In the formula, q is the linear load of pile, and P is the concentration force of the pile, σ is the stress, ε is the strain of the pile, Ac is the cross-section of pile body, γ is the weight of the anti-sliding pile. Since the test is restricted by the environment, the research can hardly meet the requirements that the weight of the model pile is 6 times than the weight of the prototype. However, in the test, most of the load the pile undertake is horizontal, thus, the weight of the pile make little influence to the results, which means that this influence can be ignored in research.

2.3 Testing Equipment

(1)Coupling tester of tunnel and slope. The size of model box is 6.3m (length)×0.7m (width)×3m (height), and the horizontal length of the slope is 4.3m.
(2)DH3816 static strain digital data acquisition system. The DH3816 static strain digital data acquisition system is of high sensitivity and low drift, and can achieve goals by multipoint circularly sampling.
(3)Strain type soil pressure mini-sensor, short for soil pressure cell. The one used in the test is a disc shape, the diameter is 28mm, the thickness is 10mm. The soil pressure cell's layout is shown as Figure 1.
(4)Strain gauge, use for measure strain gauges of pile body, the layout is shown as Figure 2.

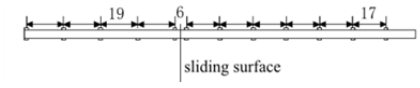

Figure 1: layout of the soil pressure cell

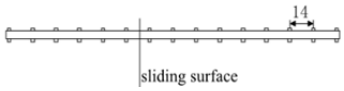

Figure 2: layout of the strain gauge

2.4 Slope Model and Parameter Determination

The external diameter of round steel pipe is 48mm, the wall thickness is 2mm, and the length is 2m. By the similar ratio of the model test, the external diameter of prototype pile is 288mm, the wall thickness is 12mm, and the length is 12m. Single row steel pipe anti-slide pile's layout is shown as Figure 3, it's slope model is shown as Figure 4.

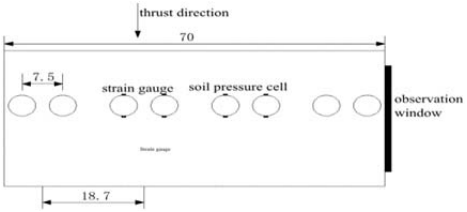

Figure 3: layout of the anti-sliding pile

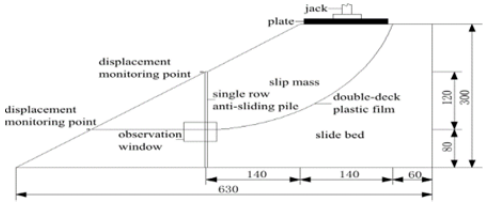

Figure 4: slope model

2.5 Model Making

(1) slide bed and slip mass. The mock object in the model test is homogeneity soil slope, slide bed and slip mass are using Chongqing's local clay as filling material. In order to make sure the embankment slope' s soil mass are dense and well-distributed, layering filling, punning solid and control each layer solid's quality have to be taken into action. In order to insure it is comparable between different test, eliminate solid moisture content's change affect test results.
(2) sliding surface. Spread out double-deck plastic film on the slide bed to stimulate slip surface.

2.6 Loading Design

This model research uses 1000t jack to apply vertically load by computer, and in the order of 50,100,…,250,300,330,…,510,540,560,…,660,670,…,730,740kN. Collecting the data when reading system become stable after each level's loading completed.

3. The Analysis of The Test Results

3.1The Analysis of The Phenomenon About The Destruction

When the load was small, the pile leaned forward, but the sliding body didn't separate with the head of the pile. During the research, when the load reached 420kN, there was a tiny transverse cracks forming in the sliding body close to the to the pile top. When loaded to 480kN, the top of the pile and the sliding body began to separate with each other, producing a pumping area. Besides, when the process of load ended and the load was 750kN, the width of the pumping area reached 8cm, and the depth was 40cm, as shown in the Figure 5. By excavating the slope, the researcher found that behind the pile, the anchorage section near the sliding surface separated with the sliding bed, producing another pumping area.

When the load was small, there was a slow subsidence of the sliding body caused by extrusion, and there was no displacement between the pile and the cut exports. However, with the increasing of the load, the displacement between the cut exports and the pile began to increase rapidly. Thus, it shows that the sliding body has slide down along the preset sliding surface integrally. The overall destruction of landslide was shown in the Figure 6. What's more, as the growing of the load, downhill side started to produce the vertical cracks and became gradually wide. At the end of the load, the vertical cracks reached 1cm wide.

Through the observation window, the research found that the pile near the sliding surface will lean forward a little, but there's no apparent bending deformation observed during the test. Besides, the research began to excavate the slope. During the test, the position of the pile which has deformation will be recorded. Then, it shows that the location of the biggest deformation of the pile was in above about 45 cm and about 20 cm below the sliding surface, where was 125cm and 60cm height in the pile.

Figure 5: Pumping area in the top of pile

Figure 6: OCrall destruction of landslide

3.2The Analysis of The Displacement Distribution Rule

The horizontal displacement-load curve of the top of the single row steel pipe anti-sliding pile was shown in the Figure 7. From the Figure 7, it demonstrates that this curve has two projecting points, they are the P=420kN and P=540kN. Since the pile has been loaded up to 200kN, it began to appear horizontal displacement. When $P \leq 420kN$, the horizontal displacement at the top of the pile started to grow slowly, with the increase of the load. Further, when $420kN \leq P \leq 510kN$, the displacement increased rapidly. At last, when $P \geq 540kN$, the rate of growing slowed down a bit.

The horizontal displacement-load curve of the cur export of the single row steel pipe anti-sliding pile was shown in the Figure 8. Again, from the Figure 8, it can also demonstrate that this curve has two projecting points, they are the P=480kN and P=560kN. When the pile loaded up to 300kN, it began to appear horizontal displacement. When $P \leq 480kN$, the horizontal displacement at the cut export of the pile started to grow slowly, with the increase of the load. Further, when $480kN \leq P \leq 540kN$, the displacement increased rapidly. At last, when $P \geq 560kN$, the rate of growing slowed down a bit.

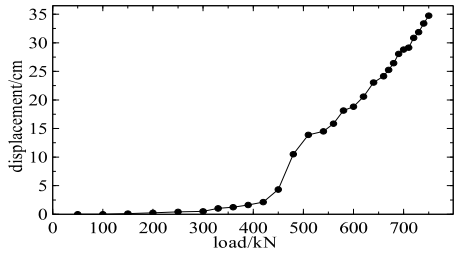

Fiurer 7: Horizontal displacement-load curve of the top of the single row steel pipe anti-sliding pile

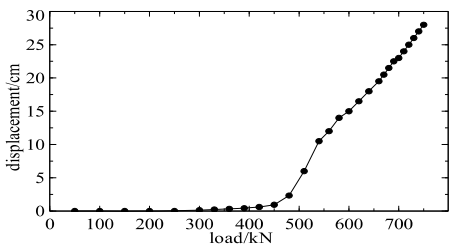

Figure 8: Horizontal displacement-load curve of the cur export of the single row steel pipe anti-sliding pile

By comparing the Figure 7 and Figure 8, the generated time of both two projecting points of pile-top is earlier than the time of the cut export. Moreover, under the same load, the horizontal displacement of the pile top is more apparent and bigger than the horizontal displacement of the cut pile.

3.3The Analysis of The Bending Moment Distribution Rule of The Pile

Pasting the strain gage in the front and behind of the anti-sliding pile during the test, the research can measure the strain of the pile. The bending moment can be obtained by using the Formula (1) by the bending theory in material mechanics.

$$M = EI(\varepsilon_y + \varepsilon_l)/d \tag{1}$$

In the formula, M is the bending moment of the measuring point, EI is the bending stiffness of pile, ε_y, ε_l are the compressive strain and tensile strain, d is the outside diameters of the anti-sliding pile. In this paper, the steel pipe material is Q235, modulus of elasticity is 206 GPa. According to the size of the steel tube, the moment of inertia can be calculated, which is 4.077cm^4. The research considers both the bending moment to pile back in tension as positive and the tension of the side as negative.

The bending moment distribution of the single row steel pipe anti-sliding pile when under different loads is shown in the Figure 9.

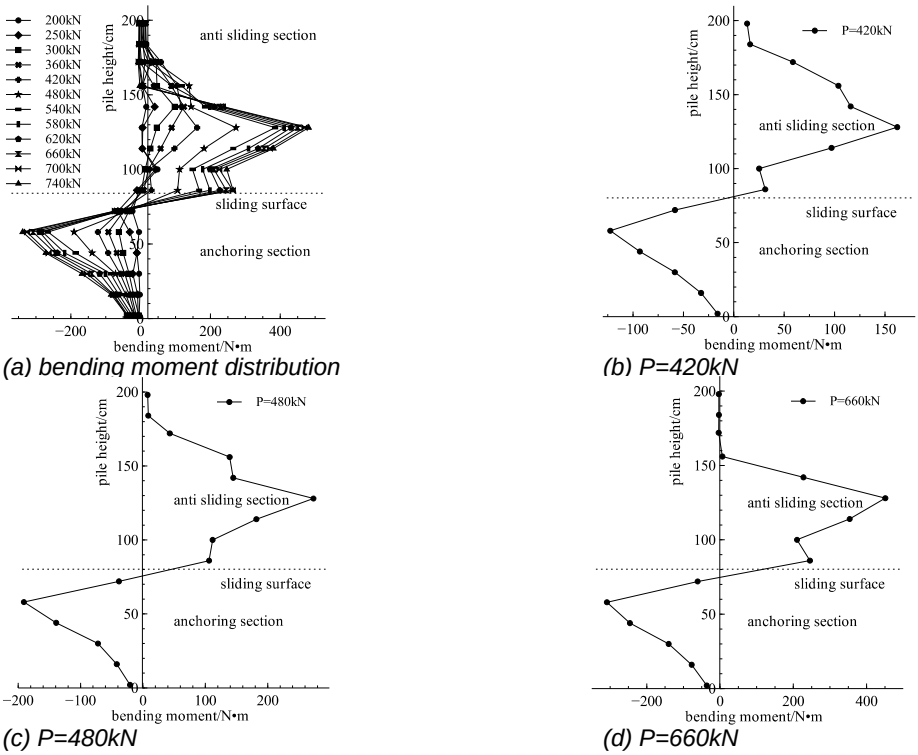

(a) bending moment distribution *(b) P=420kN*

(c) P=480kN *(d) P=660kN*

Figure 9: Bending moment distribution of single row steel pipe anti-sliding pile when under different loads

From the Figure 9(a), it can be known that,

(1) The bending moment of the single pile distributed in apparent anti-S. When P $\leq$ 360kN, the zero point of the bending moment is located about 5 cm above the sliding surface, where is 75cm height in the pile. When P=420kN, the zero point of the bending moment is located at the sliding surface, where is 80cm height in the pile. When P $\geq$ 480kN, the zero point of the bending moment is located about 5 cm beneath the sliding surface, where is 80cm height in the pile. Thus, all these results showed that with the increase of the load, the position of the zero point of the bending moment gradually move up to down.

(2)the maximum bending moment is greater than the maximum negative moment, which means that the maximum bending moment of against sliding is greater than the maximum bending moment of the anchoring.

(3) The maximum positive bending moment is located about 48 cm above the sliding surface, where is 128cm height in the pile. The maximum negative bending moment is located about 22 cm beneath the sliding surface, where is 58cm height in the pile.

(4) When $P \leq 420$kN, the values of positive and negative bending moment of pile increase constantly and the margins are small. The increase was significantly bigger when P=480kN and P=540kN, but when $P \geq 580$kN, the increase apparently became smaller.

From the Figure 9(a)-(d), it shows that,

(1) The bending moment in the top of the pile gradually decrease when $P \geq 480$kN, which has conformity with the phenomenon that when the load is big, there is pumping area generated in the back of the pile.

(2) As the growing of the load, the area of zero moment became bigger which shows that with the increasing of the load, the pumping area of the back of the anti-sliding pile gradually also became bigger.

(3) Under the load that P=660kN, the bending moment of pile is close to zero in the scope of 44cm, which is consistent with the phenomenon that when P=660kN, the depth of the pumping area is about 40cm. Besides, when $P \geq 660$kN, the scope of the bending moment closed to zero didn't grow any more.

3.4The Analysis of The Soil Pressure Distribution Rule of The Pile

The soil pressure of the single row anti-sliding pile under different loads is shown in the Figure 10. From the Figure 10(a),(b), the research shows that,

(1) The maximum value of the soil pressure of anti-sliding section in front of the pile located in about 70cm above the sliding surface, where is the 150cm height of the pile. The maximum value of the soil pressure of the anchoring section in front of the pile is in the nearby of the sliding surface, but the value is approximately zero in the bottom.

(2) The maximum value of the soil pressure of anti-sliding section in back of the pile located in about 40cm above the sliding surface, where is the 120cm height of the pile. Besides, the bottom of the pile has the biggest pressure of the anchoring section in back of the pile, however, near the sliding surface, this value is close to zero, which demonstrates the consistence with the appearance of pumping area.

(3) The maximum soil pressure of the front anchoring section is bigger than the value of the anti-sliding section. However, the maximum soil pressure of the back anchoring section is smaller than the value of the anti-sliding section.

(4) Since the load was growing bigger and bigger, the soil pressure in the front of the anti-sliding section also became bigger. When P=200kN and P=300kN, the growing rate turned into faster, but when P>300kN, the rate became slower; Moreover, the soil pressure in the front of anchoring section grew with the growing of the load. When $P \leq 420$kN, it is close to an approximate constant increase and its margins are small. When P=480kN, the growing margins began to increase, the margin was really big when P=540kN, however, this margin turned to small when $P \geq 580$kN.

(5) Behind the pile, the soil pressure in the anti-sliding section grew with the growing of the load. When $P \leq$ 420kN, it is close to an approximate constant increase and its margins are small. When P=480kN and P=540kN, the growing margins began to increase apparently. However, when $P \geq 580$kN the margin became much smaller, and the pressure in anchoring section grew more slowly with the growing load.

(6) In the anchoring section and the back of the pile, where have less soil pressure are exactly the location with bigger soil pressure in the front of the anti-sliding section. Nevertheless, in the front of the pile and the anchoring section, where have less soil pressure are also exactly the place with bigger soil pressure in the back of the anti-sliding section. Moreover, it obviously shows that in the front of the pile, the rule of distribution of the soil pressure apparently opposites with the rule in the back of the pile.

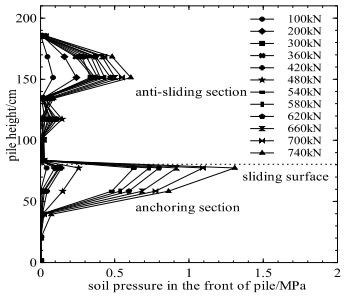

(a)soil pressure distribution in the front of pile

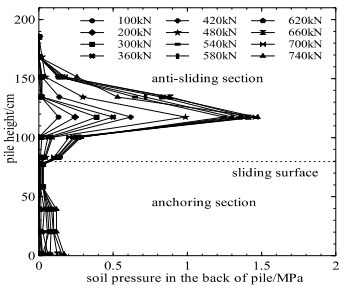

(b)soil pressure distribution in the back of pile

Figure 10: Soil pressure distribution of single row steel pipe anti-sliding pile when under different loads

4. Conclusion

(1)During the test, the pile back began to separate with the sliding body gradually. Furthermore, the anchoring section in the back of pile near the sliding surface separated with the slope bed, generating a pumping area.
(2)When the load is up to 420kN, the horizontal displacement in the top of the pile began to increase rapidly, when the load became 480kN, the horizontal displacement of the cut export also grew rapidly
(3)The bending moment of the pile distributed in apparent anti-S, the zero point of the bending moment is located near the sliding surface. The maximum moment of the anti-sliding section is in the place 48cm above the sliding surface. The maximum moment of anchoring section is located under the surface about 22cm deep. The maximum moment of the anti-sliding section is bigger than the value of the anchoring. Furthermore, both the back of the anti-sliding section and the front side of anchoring section are carrying loads in tension.
(4)The maximum soil pressure in front of the anti-sliding pile is located in 70cm above the sliding surface. The maximum soil pressure of the anchoring section is near the surface, but this value is zero in the bottom of the pile. In the back of the anti-sliding pile, the maximum soil pressure is in the 40cm above the surface. The soil pressure is bigger in the anchoring section, and the value in the surface is zero. The maximum soil pressure of the front anchoring section is bigger than the value of the anti-sliding section. However, the maximum soil pressure of the back anchoring section is smaller than the value of the anti-sliding section. The rule of distribution of the soil pressure apparently opposites with the rule in the back of the pile.

References

Ashour M, Ardalan H(2012). Analysis of pile stabilized slopes based on soil–pile interaction. Comput Geotech 39: 85-97. doi:10.1016/j.compgeo.2011.09.001

Xu Jian-cong, Niu Fu-sheng(2014). Safety factor calculation of soil slope reinforced with piles based on Hill's model theory[J]. Environ Earth Sci, 71(8): 3423-3428. doi: 10.1007/s12665-013-2730-3.

Bruce D A, Cadden A W, Sabatini P J(2005). Practical advice for foundation design-micropiles for structural support[C]// GSP 131 Contemporary Issues in Foundation Engineering, ASCE. [S.1.]: [s.n.]: 1-25. doi: 10.1061/40777(156)14.

Zhang Xu, Tan Ju-hong (2013). Research on Majiagou Landslide Stability Analysis and Control Design[C]. Proceedings of the 2012 International Conference on Cybernetics and Informatics, Lecture Notes in Electrical Engineering 163. New York, 595-602. doi: 10.1007/978-1-4614-3872-4_76.

Yan Jin-kai, Yin Yue-ping, Men Yu-ming(2009). Model Test Study on Landslide Reinforcement with Single Micropile[J]. Journal of Engineering Geology, 17(5): 669-674. doi: 10.3969/j.issn.1004-9665.2009.05.015.

Gong Jian, Chen Ren-peng, Chen Yun-ming, et al(2004). Prototype testing study on micropiles under lateral loading[J]. Chinese Journal of Rock Mechanics and Engineering, 23(20): 3541-3546. doi: 10.3321/j.issn:1000-6915.2004.20.027.

Poulos H G, Chen L T, Hull T S(1995). Model tests on single piles subjected to lateral soil movement[J]. Soils and Foundations, 35(4), 85-92. doi: 10.3208/sandf.35.4_85.

Xin Jian-ping, Zheng Ying-ren, TANG Xiao-song(2014). Research on Failure Mechanism of Anti-sliding Micropiles Based on Elastoplastic Model[J]. Chinese Journal of Rock Mechanics and Engineering, 33(S.2): 4113-4121. doi: 10.13722/j.cnki.jrme.2014.s2.089.

Kong Ji-ming, Cai Qiang, Zhang Yin, et al(2013). Physical Model Test of Debris Landslide Reinforcement with Single Row Micro-pile[J]. Journal of Mountain Science, 31(4): 399-405. doi: 10.3969/j.issn.1008-2786.2013.04.003.

Li Xun-chang, Men Yu-ming, He Guang-yu(2009). Test research on strata resistance of pile slide of anchor anti-slide pile[J]. Rock and Soil Mechanics, 30(9): 2655-2659. doi: 10.3969/j.issn.1000-7598.2009.09.019.

IAI S(1989). Similitude for shaking table test on soil-structure-fluid model in l-g gravitational field[J]. Soils and Foundations, 29(1): 105-118. doi: 10.3208/sandf1972.29.105.

Lei Wen-jie, Zheng Ying-ren, WANG Gong-xian, et al(2007). Mechanism analysis of slope reinforcement with deeply buried piles with model test[J]. Chinese Journal of Rock Mechanics and Engineering, 26(7): 1347-1355. doi:10.3321/j.issn:1000-6915.2007.07.006.

Zhou Wei-yuan, Yang Ruo-qiong, Liu Yao-ru, et al(2005). Research on geomechanical model of rupture tests of arch dams for their stability[J]. Journal of Hydroelectric Engineering, 24(1): 53-5. doi: 10.3969/j.issn.1003-1243.2005.01.008.